Journal of Theoretical Biology 442 (2018) 139–148

Contents lists available at ScienceDirect

Journal of Theoretical Biology

journal homepage: www.elsevier.com/locate/jtbi

No appendix necessary: Fecal transplants and antibiotics can resolve *Clostridium difficile* infection

Tejas Joshi[a,*], Bret D. Elderd[b], Karen C. Abbott[c]

[a] Feinberg School of Medicine, Northwestern University, 303. East Chicago Ave., Chicago, IL 60611, USA
[b] Department of Biological Sciences, Louisiana State University, Baton Rouge, LA, USA
[c] Department of Biology, Case Western Reserve University, Cleveland, OH, USA

ARTICLE INFO

Article history:
Received 6 August 2017
Revised 4 December 2017
Accepted 15 January 2018

Keywords:
Microbiome
Bistability
Mathematical approach
Gut alternative steady states

ABSTRACT

The appendix has been hypothesized to protect the colon against *Clostridium difficile* infection (CDI) by providing a continuous source of commensal bacteria that crowd out the potentially unhealthy bacteria and/or by contributing to defensive immune dynamics. Here, a series of deterministic systems comprised of ordinary differential equations, which treat the system as an ecological community of microorganisms, model the dynamics of colon microbiome. The first model includes migration of commensal bacteria from the appendix to the gut, while the second model expands this to also include immune dynamics. Simulations and simple analytic techniques are used to explore dynamics under biologically relevant parameters values. Both models exhibited bistability with steady states of a healthy state and of fulminant CDI. However, we find that the appendix size was much too small for migration to affect the stability of the system. Both models affirm the use of fecal transplants in conjunction with antibiotic use for CDI treatment, while the second model also suggests that anti-inflammatory drugs may protect against CDI. Ultimately, in general neither the appendiceal migration rate of commensal microbiota nor the boost to antibody production could exert an appreciable impact on the stability of the system, thus failing to support the proposed protective role of the appendix against CDI.

1. Introduction

With the advent of novel metagenomic tools to study the human microbiome, the importance of beneficial symbiont-host interactions in human health has rapidly become evident. Abundant microbial species, which reside primarily in the gastrointestinal tract, play critical roles in maintaining the health of their ecosystem, the human body, by freeing energy from otherwise inaccessible dietary substrates, regulating the immune system and protecting the host from invasion by pathogens (Dethlefsen et al., 2007). Recent studies have linked imbalances in microbiome compositions to chronic conditions as diverse as inflammatory bowel disease, obesity, and type 2 diabetes (Flint, 2011; Larsen et al., 2010; Sahami et al., 2015). Thus, maintaining a properly functioning microbiome appears essential for human health.

The adult intestinal microbiota is a relatively resilient ecosystem with a composition that is quite stable over time (Bucci et al., 2012). However, external disturbances, such as a dramatic change in diet or an antibiotic regime, can shift this composition, moving the community to an alternative state. These changes may affect the gut's functionality or induce susceptibility to disease (Costello et al., 2012). For example, sustained antibiotic use kills commensal bacteria and provides a niche opportunity for the pathogenic *Clostridium difficile* bacteria. This may lead to *C. difficile* infection (CDI), the leading cause of U.S. hospital-acquired diarrhea with up to 300,000 cases annually (Rupnik et al., 2009). Although incidences vary greatly between countries, CDI is a growing health care problem in the Western world with recent increases in both the numbers of cases and the CDI-associated mortality rate (Lessa et al., 2015; McDonald et al., 2006; Rupnik et al., 2009).

CDI threatens the function of health care systems by increasing hospitalization costs and posing the constant threat of spread. Clinically, CDI leads to a large span of outcomes from mild diarrhea to fulminant, life-threatening colitis that requires surgical intervention. Even relatively benign presentations of CDI significantly increase the length of admissions and morbidity and mortality rates (Seretis et al., 2014). Patients with recurrent CDI have a 33% higher hazard of death in the following nine months as compared to patients without recurrent CDI (Olsen et al., 2015). Furthermore, recurrence of CDI following the resolution of primary infection is a

* Corresponding author.
E-mail addresses: tejas.joshi@northwestern.edu (T. Joshi), elderd@lsu.edu (B.D. Elderd), karen.abbott@case.edu (K.C. Abbott).

https://doi.org/10.1016/j.jtbi.2018.01.013
0022-5193/

complication in 19–20% of patients (Johnson, 2009). These effects have been associated with the emergence of highly virulent and antibiotic resistant strains of *C. difficile* (Spigaglia, 2016).

It has been suggested that the appendix may protect against CDI by introducing bacteria into the gut that compete with *C. difficile* or by contributing to the anti-CDI immune response. A retrospective study of 396 patients found that the presence of an appendix was significantly negatively associated with CDI recurrence (Im et al., 2011). However, another retrospective study found no such significant difference (Khanna et al., 2013). The evidence is therefore unclear as to whether these hypothesized protective effects do exist. Further observational studies are needed to clarify whether appendix presence is protective against CDI recurrence (Seretis et al., 2014). Meanwhile, we take a complementary approach here and ask whether the mechanisms through which the appendix is thought to be protective are theoretically strong enough to have the proposed effect.

Understanding effects of the appendix on the colon microbiome requires a study of the pairwise interactions of hundreds of species present in the human gut, including commensal, mutualistic, competitive and exploitative elements (Coyte et al., 2015). These interactions include direct action through secretion of toxins, competition for limited space and resources, and more complex mechanisms such as immune system modulation (Stein et al., 2013). Ecological theory is ideally suited to tackle the problem of simulating these complex, interspecies interactions (Costello et al., 2012). Using techniques from theoretical ecology, we may produce and analyze relatively simple models that can exhibit complex phenomena such as multi-stability or chaotic behavior (Petraitis, 2013). These microbiome-based models can lend important insight into whether the appendix serves a significant function in protecting a healthy microbiota state of the gut.

Here, we introduce a series of simple ecological models of the appendix and gut microbiota to characterize the relationship between the appendix and CDI. This allows us to ask whether the appendix can be considered a microbial source or the source of an immune response that shifts the perturbed system back to a balanced microbiome. We also investigate the impact of appendix presence on standard treatments—antibiotics and fecal transplants—for CDI. Our findings do not support the role of appendiceal 'reseeding' of the colon through migration or of appendiceal antibody production as a significant factor in preventing this infection. However, the use of antibiotic treatments and fecal transplants are well supported by the models.

1.1. Study system

The *Clostridium difficile* bacterium is a gram-positive, spore-forming anaerobic bacillus that resides environmentally and is found in the stools of 5% of healthy adults and 30–70% of infants (Kachrimanidou and Malisiovas, 2011). *C. difficile* associated disease can arise if the normal gut flora has been disrupted, particularly by antibiotic therapy. When the colonization barrier formed by the gut microbiome is compromised, endogenous or exogenous (through the fecal-oral route) contamination by spores may occur. After colonization, the main clinical symptoms and signs of CDI, secretory diarrhea and inflammation of the colonic mucosa, are largely explained by the bacterias release of the enterotoxin Toxin A (TcdA) and the cytotoxin Toxin B (TcdB) (Rupnik et al., 2009). However, the loss of commensal bacteria also worsens inflammation (Solomon, 2013).

Commensal intestinal microflora protect against CDI directly through competition for nutrients, physical occupation of mucosal sites and the production of antimicrobial peptides (Buffie and Pamer, 2013). The indirect role of commensal bacteria in mediating inflammation has recently been clarified. Dendritic and epithelial cells contain signaling modules such as toll-like receptors that continually sample the lumen for bacterial-derived contents (Chieppa et al., 2006). The detection of molecules from commensal bacteria lessens inflammation in two ways: by inducing the growth of microbe-induced regulatory T cells (iTregs) and by suppressing the growth of proinflammatory T helper 17 (Th17) T cells in the lamina propria—the immune cell-rich connective tissue layer lining the gut. This mechanism maintains intestinal homeostasis (Solomon, 2013). During antibiotic therapy, the loss of commensal flora thus decreases the iTreg:Th17 balance in the lamina propria and causes mild inflammation.

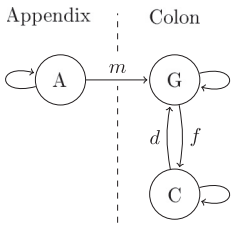

Fig. 1. General structure of three state system for *A* (commensal bacteria in the appendix), *G* (commensal bacteria in the colon) and *C* (*C. difficile* bacteria in the colon): arrows depict direct interactions and edge labels are parameters involved in that interaction (See text for details).

It has been suggested that the appendix serves as a safe house for commensal bacteria due to its production of mucins and secretory immunoglobulin A (IgA), both of which enhance the survival of those bacteria in a biofilm. The narrow lumen of the appendix as well as its location at the lower end of the cecum protect its contents from potential pathogens in the fecal stream. Therefore, the regular shedding of normal enteric bacteria from the appendix may serve as a potential source of commensal bacteria to reseed the colon in the event of CDI (Bollinger et al., 2007).

Furthermore, it has been proposed that the presence of the appendix is protective against recurrence of CDI due to its abundance of gut associated lymphoid tissues (GALT). The appendiceal GALT contains a higher density of immunoglobulin IgA- and IgG-producing immunocytes than the colon, and animal models demonstrate that the removal of the appendix leads to decreased immunoglobulin production (Johnson et al., 1995). Experimental evidence highlights the role of these antibodies against CDI. During recurrent CDI, humoral immune responses appear largely characterized by serum IgG against TcdA (Im et al., 2011). Additionally, lower levels of fecal IgA against TcdA have been found in recurrent CDI patients as compared to single-episode CDI (Johnson et al., 1995). Finally, serum IgA, although not IgG, against TcdA is expressed in high levels in the convalescence phase after CDI in one third of patients. Therefore, it has been hypothesized that the TcdA released during CDI stimulates the growth of appendicular B cells that then produce IgG and IgA to protect against infection (Im et al., 2011).

Here, our first model will only evaluate the migration-hypothesis (Section 2). The second model will build on the first to also incorporate the effects of the appendix on inflammation and antibody production (Section 3).

2. Migration model

We first ignore inflammatory dynamics and consider the system in which the appendix only acts on the colonic microbiome via migration. Appendiceal bacteria (A) are taken as a single class that contribute to the growth of colonic 'good' bacteria (G). Those commensal bacteria compete with *C. difficile* bacteria (C) for resources (see Fig. 1).

Table 1
Equilibria of the migration model (6)–(7) and their stability. All solutions are finite as long as $df \neq 1$, which we assume here. The stability criteria are identified in Appendix D. Entries with a dash (-) are omitted here due to their complexity, but are available in the supplementary materials (See Appendix F).

Equilibria	Expression (C, G)	Nonnegative criteria	Stability criteria
$e1$	$\left(0, \frac{l}{2} - \frac{\sqrt{l}\sqrt{4m\bar{A}+ly}}{2\sqrt{y}}\right)$	$m\bar{A} = 0$	Never
$e2$	$\left(0, \frac{l}{2} + \frac{\sqrt{l}\sqrt{4m\bar{A}+ly}}{2\sqrt{y}}\right)$	Always	$f \geq 1$ or $f < 1$ and $y < \frac{fm\bar{A}}{(1-f)l^2}$
$e3$	$\left(\frac{l\sqrt{y}(df+f-2)+f\sqrt{l}\sqrt{m\bar{A}(4-4\ df)+(d-1)^2ly}}{2\sqrt{y}(df-1)}, \frac{(d-1)l\sqrt{y}-\sqrt{l}\sqrt{m\bar{A}(4-4df)+(d-1)^2ly}}{2\sqrt{y}(df-1)}\right)$	–	–
$e4$	$\left(\frac{l\sqrt{y}(df+f-2)-f\sqrt{l}\sqrt{m\bar{A}(4-4\ df)+(d-1)^2ly}}{2\sqrt{y}(df-1)}, \frac{(d-1)l\sqrt{y}+\sqrt{l}\sqrt{m\bar{A}(4-4\ df)+(d-1)^2ly}}{2\sqrt{y}(df-1)}\right)$	–	–

The time-evolution of these variables is given by the following set of three coupled differential equations:

$$\frac{dA}{dt} = xA\left(1 - \frac{A}{k}\right) - mA \tag{1}$$

$$\frac{dG}{dt} = yG\left(1 - \frac{G + dC}{l}\right) + mA \tag{2}$$

$$\frac{dC}{dt} = zC\left(1 - \frac{C + fG}{l}\right) \tag{3}$$

where x, y and z are maximum growth rates of commensal bacteria in the appendix and colon and of *C. difficile* respectively, k and l are the carrying capacities of the appendix and colon respectively, m is the appendiceal migration rate, and d and f are competition coefficients. These equations adapt a classic analysis of two ecological competitors in two spatial patches by DeAngelis et al. (1979) to the gut microbiome. The first term in each equation describes logistic growth for that bacterial class and the $-dCG$ and $-fCG$ terms account for the competition between species in the colon. The mA terms describe appendix bacterial migration to the colon.

Note that we only consider pathogenic *C. difficile* bacteria to belong in the state C. Non-pathogenic strains do not produce toxin and should not induce inflammation alone. As they are also able to indirectly compete with the pathogenic strains of *C. difficile* bacteria, we can consider them to be part of the population of good bacteria.

The appendix state Eq. (1) is a simple, first order ordinary differential equation which is easily solved. For a constant j, the explicit form is:

$$A(t) = \frac{k(m-x)}{e^{[(m-x)(t-kj)]} - x} \tag{4}$$

As $t \to \infty$, the appendix population approaches

$$\bar{A} = \begin{cases} \frac{k(x-m)}{x} & \text{if } m < x \\ 0 & \text{else} \end{cases} \tag{5}$$

For our purposes, transient appendix population dynamics are unimportant. The onset of CDI generally should not be temporally correlated with appendectomy. Therefore, we can assume that at the start of CDI, the patient will either have an appendix with a bacterial population that has reached carrying capacity or no appendix. As we also assume the biologically plausible condition that $m < x$, that is that the appendix migration rate is smaller than the bacterial growth rate in the appendix, we set the appendix population constant to its nonzero equilibrium value. The migration-only model thus reduces to two equations.

$$\frac{dG}{dt} = yG\left(1 - \frac{G + dC}{l}\right) + m\bar{A} \tag{6}$$

$$\frac{dC}{dt} = zC\left(1 - \frac{C + fG}{l}\right) \tag{7}$$

Note that we can model appendix absence by setting $m = 0$. This system may be non-dimensionalized (Appendix A), but for ease of interpretation, we present our analyses in terms of this dimensional model.

2.1. Steady states and stability

Before discussing the equilibria, we note that the system (6)–(7) is always non-negative, bounded and non-oscillatory, given non-negative initial conditions (See Appendix B for details).

In general, the migration model has 4 steady-state solutions that we name $e1$ through $e4$ (Table 1). Notice that in the presence of migration, $e1$ has a negative population.

In the special case when $df = 1$ and $d \neq 1$, then instead of equilibria $e3$ and $e4$, there exists a single steady state with populations $(C, G) = (l - \frac{m\bar{A}}{d(d-1)y}, \frac{m\bar{A}}{(d-1)y})$. This equilibrium is the limiting value of both $e3$ and $e4$ as $df \to 1$, so without loss of generality our analyses will focus on $e3$ and $e4$ in the $df \neq 1$ case.

We note that in the absence of migration ($m\bar{A} = 0$), the system (6)–(7) reduces to the standard Lotka–Volterra model of two species competition. In this case, $e1$ becomes the $(0, 0)$ equilibrium while $e2$ and $e3$ reduce to equilibria of the form $(C, G) = (0, \bar{G})$ and $(C, G) = (\bar{C}, 0)$ respectively for non-zero carrying capacities $\bar{C}$ and $\bar{G}$, and $e4$ reduces to the coexistence equilibrium.

2.2. Short- and long-term bacterial dynamics

Model parameters used in this article are summarized in Table 2 and more details follow in Appendix C.

Under this parameterization, the system exhibits bistability. Fig. 2 depicts an example of the switch in long-term behavior between an equilibrium with good bacteria dominant and one in which *C. difficile* is dominant in the colon, driven by a change in initial conditions.

Notably, increasing the total amount of migration can theoretically switch the system from the bistable structure to a monostable structure (Fig. 3). Note from Table 1 that sufficiently large appendix sizes, which are directly proportional to $m\bar{A}$, force $e1$, $e3$, and $e4$ to each contain at least one negative or imaginary population. As the system is non-negative, bounded and non-oscillatory (Appendix B), every non-negative initial condition must then converge to the single positive equilibrium $e2$.

For example, assume the system is bistable with an appendix size which we steadily increase. Then, $e1$ has a negative population, so the remaining three equilibria must be real and positive.

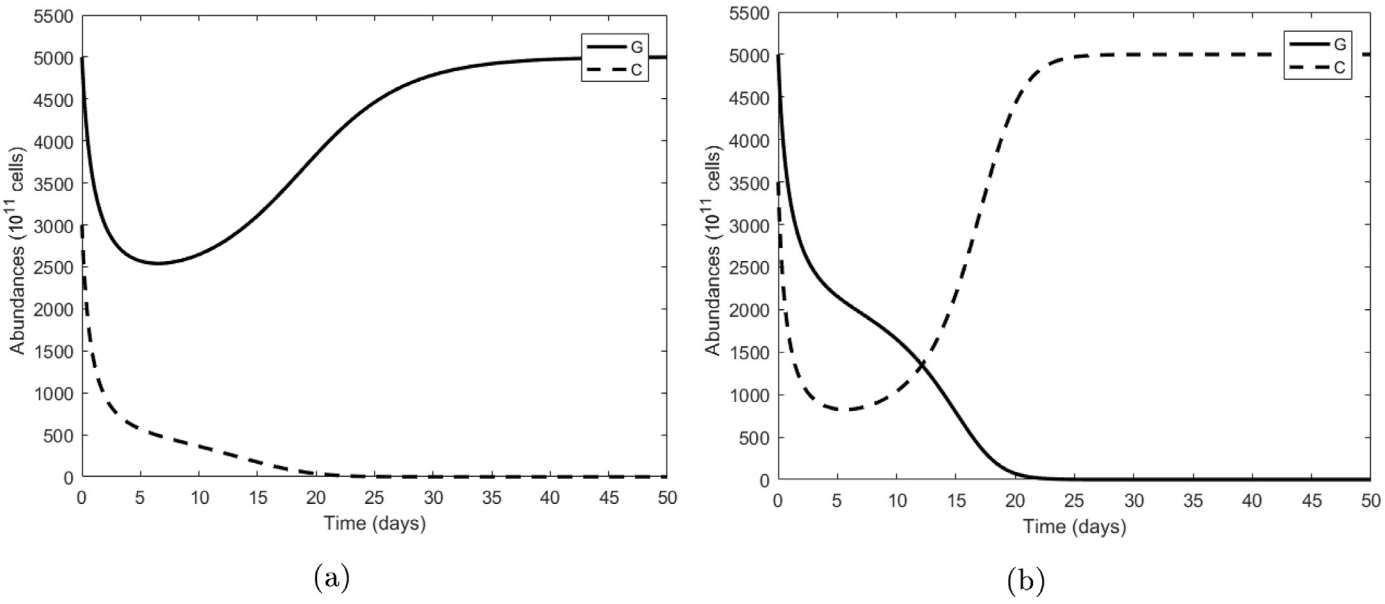

Fig. 2. Bacterial populations over time with two different initial conditions with parameters as given in Table 2. Panel (a) uses initial conditions of $C(0) = 3 \cdot 10^3$ (representing an initial population of $3 \cdot 10^{14}$ cells), $G(0) = 5 \cdot 10^3$ and depicts the extinction of *C. difficile* in the colon. Panel (b) uses initial conditions of $C(0) = 3.5 \cdot 10^3$, $G(0) = 5 \cdot 10^3$ and depicts the near extinction of good bacteria in the colon, in which a slightly positive population is maintained by migration from the appendix.

Table 2
Table summarizing the parameters that appear in models (6)–(7), (8)–(12) and their values used throughout the numerical simulation. The elements in the Value column show the specific values used in simulation (in parentheses) as well as the ranges over which we varied those values in sensitivity analyses. For our parameterization, C and G have units of 10^{11} bacteria, T and B have units of fmol (10^8 molecules) and I is unitless. Note that several parameter values are based on reasonable estimates and so these values vary widely in the sensitivity analysis to account for this uncertainty (See Appendix C).

Param.	Description	Value	Units	Ref
x	Maximum growth rate of appendiceal bacteria	0.2 – 0.3 (0.3)	per capita day^{-1}	Park et al. (2016)
y	Maximum growth rate of colonic bacteria	0.2 – 0.3 (0.2)	per capita day^{-1}	Park et al. (2016)
z	Maximum growth rate of *C. difficile*	0.1 – 0.9 (0.75)	per capita day^{-1}	Estimate
m	Migration rate of bacteria from appendix to colon	0 – 0.3 (0.2)	per capita day^{-1}	Estimate
k	Appendix carrying capacity	1 – 10 (5)	10^{11} bacteria	Estimate
l	Colon carrying capacity	$10^3 - 10^4$ ($5 \cdot 10^3$)	10^{11} bacteria	Tancrede (1992)
d	Competition acting on colonic bacteria	0 – 10 (5)	per capita day^{-1}	Estimate
f	Competition acting on *C. difficile*	0 – 10 (2)	per capita day^{-1}	Estimate
Parameters added for analysis of Model 2.				
q_G	Rate of inflammation-mediated killing of good bacteria	0 – 10 (1)	day^{-1}	Estimate
q_C	Rate of inflammation-mediated killing of *C. difficile*	1 – 10 (5)	day^{-1}	Estimate
n	Rate of toxin production	$10^{-2} - 10^{-1}$ (10^{-2})	fmol day^{-1}	Albinsson et al. (2014)
α	Relative effect of toxin on inflammation	1 – 100 (10)	–	Estimate
β	Relative effect of *C. difficile* bacteria on inflammation	1 – 100 (100)	–	Estimate
ξ	K_a for antibody-antigen binding	$10^{-6} - 10^{-5}$ ($5 \cdot 10^{-6}$)	fmol^{-1} day^{-1}	Zhuang et al. (2001)
χ	Max rate of antibody production	$10^9 - 10^{11}$ ($3 \cdot 10^{10}$)	fmol day^{-1}	Alberts et al. (2002)
h_I	Inflammation decay rate	$10^3 - 10^4$(10^4)	day^{-1}	Coxon et al. (1999); Reynolds et al. (2006)
h_T	Half-constant for toxin-induced antibody production	$10^3 - 10^6$ (10^6)	fmol	Estimate
p	Protein decay constant in colon	1.25 – 5 (2)	day^{-1}	Cremer et al. (2016)
w	Antibody production boost from appendix	0 – 1 (0.2)	–	Estimate

The system's required switch to monostability can occur only when equilibria $e3$ and $e4$ annihilate or both become negative, as equilibrium $e2$ must remain positive. However, the equilibrium expression for $e4$ makes it clear that increasing the appendix size cannot change the positivity of its population. Therefore, $e3$ and $e4$ must annihilate. By examining the condition for $e3$ and $e4$ to be equal, we find that this switch in number of equilibria occurs if and only if the appendix carrying capacity is greater than the saddle-node bifurcation value at $k = \frac{(d-1)^2 lxy}{4(df-1)m(x-m)}$.

However, for the standard parameter set given in Table 2, this requires an appendix size that is over 100 times larger than our maximum estimated value, meaning that the appendix would need to house on the order of 10% of the number of bacterial cells housed in the entire colon. We view this as an unrealistic scenario given the small size of the appendix, so although migration-driven monostability is a theoretical possibility, it is not a biological one.

3. Migration-inflammation model

Next, we investigate the effects of the appendix on immune dynamics during CDI. We expand the migration-only model to include new state variables as depicted in Fig. 4: toxins TcdA and TcdB produced by *C. difficile (T)*, anti-toxin antibodies produced in the appendix and colon (B), and a unitless index representing the level of inflammation (I).

The time-evolution of these variables is given by

$$\frac{dG}{dt} = yG\left(1 - \frac{G + dC}{l}\right) + m\bar{A} - q_G IG \tag{8}$$

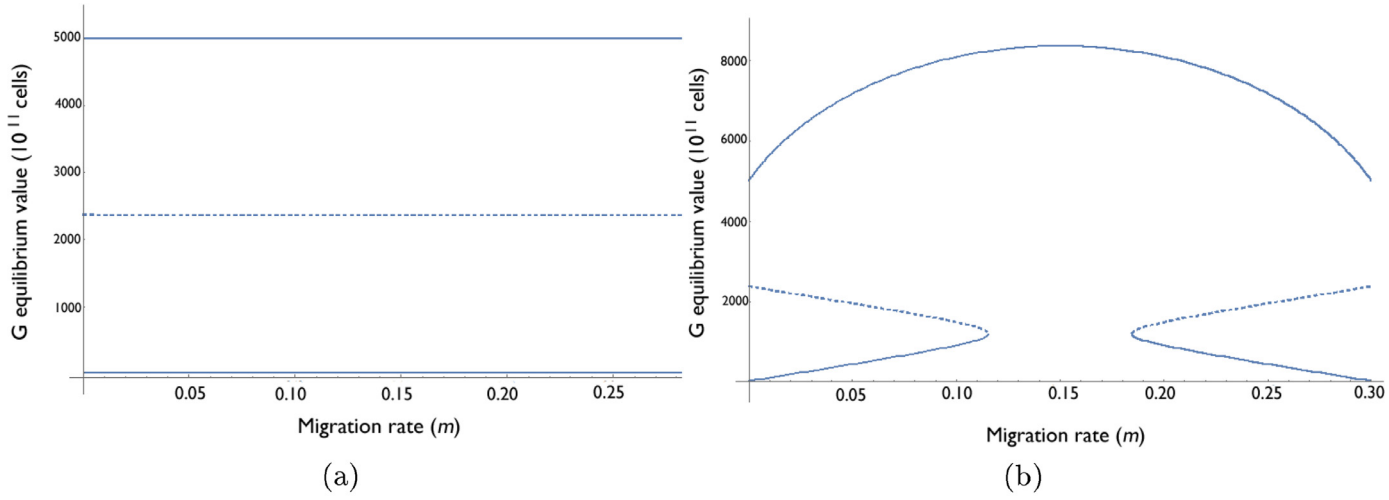

Fig. 3. Commensal bacterial equilibria as migration rate m varies across all allowable values ($0 \le m \le x$) with (a) $k = 5$ and (b) $k = 15,000$. The remaining parameter values are given in Table 2. Solid lines denote stable equilibria while dashed lines are unstable equilibria and, from top to bottom, are $e2$, $e3$ and $e4$. In (b), equilibria $e3$ and $e4$ collide in saddle-node bifurcations as m varies.

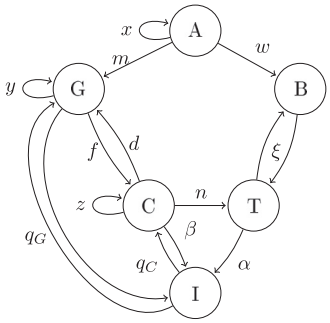

Fig. 4. General structure of model for A (commensal bacteria in the appendix), G (commensal bacteria in the colon), C (*C. difficile* bacteria), I (inflammation), T (toxin), and B (antibody): arrows depict direct interactions and edge labels are of parameters involved in that interaction (See text for details).

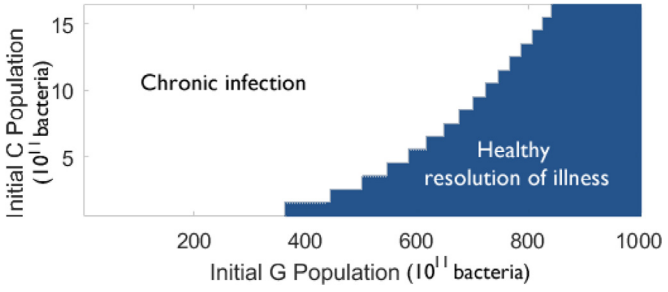

Fig. 5. The equilibria to which system (8)–(12) will converge, under the parameter set given in Table 2 as approximated by running a simulation 60 days for each initial condition and returning the final value. The line of healthy states with an initial population of $C = 0$ is omitted here.

$$\frac{dC}{dt} = zC\left(1 - \frac{C + fG}{l}\right) - q_C IC \tag{9}$$

$$\frac{dB}{dt} = (w+1)\frac{\chi T}{T + h_T} - \xi BT - pB \tag{10}$$

$$\frac{dT}{dt} = nC - \xi BT - pT \tag{11}$$

$$\frac{dI}{dt} = \left(\frac{\alpha T + \beta C}{G}\right)(1 - I) - h_I I \tag{12}$$

The description of all new parameters can be found in Table 2.

In addition to the assumptions included in system (6)–(7), we also make the following assumptions:

- The variable representing inflammation, I, is always between 0 (no inflammation) and 1 (the maximum possible value). The rate of increase in inflammation is a weighted ratio of the number of *C. difficile* bacteria and toxin molecules to good bacteria. This accounts for the ratio of signals promoting the growth of pro-inflammatory Th17 cells and anti-inflammatory iTreg cells.
- Maximal inflammation ($I = 1$) kills both good and *C. difficile* bacteria at a per capita rate of q_G and q_C respectively. Lower levels of inflammation kill both bacterial populations proportionally slower.
- Antibody is produced in a saturating dose-dependent response to exposure to toxin. The appendix boosts the antibody production rate by an additional factor of w.
- Antibody and toxin are lost due to binding with each other at a rate ξ or due to flow through the gut at a rate p. We also assume that a toxin or antibody passes through the colon by diffusion in 5–15 hours and so the natural decay of these proteins is insignificant in comparison.
- Toxin production is linear with respect to *C. difficile* population.
- Inflammation decays at a constant rate h_I.

This treatment of inflammation as a single bound variable with a saturating dose-dependent response to increasing the ratio of inflammatory agent to non-inflammatory agent is analogous to its treatment in models of necrotizing enterocolitis (Arciero et al., 2010) and uncontrolled acute inflammation (Kumar et al., 2004).

3.1. Short- and long-term dynamics

For this 5-dimensional model, we used numerical simulation to investigate behavior. Like the migration-only model, this system can also exhibit bistability between a successful resolution of CDI and chronic CDI states. For the standard parameterization given in Table 2, Fig. 5 depicts how initial condition determines which steady state is reached.

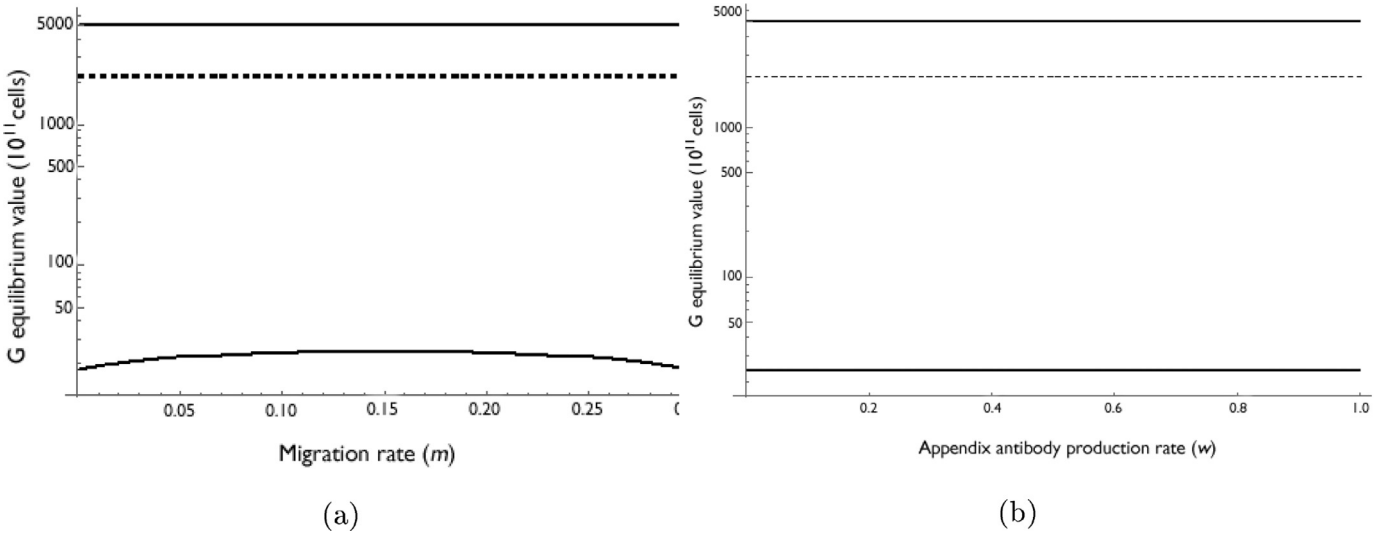

Fig. 6. A bifurcation diagram of the equilibria of G as a function of (a) migration rate m and (b) appendiceal antibody production rate w. Stable equilibria are denoted with solid lines and the unstable equilibrium with a dashed line. The equilibrium population axis has a logarithmic scale. Parameters used are given in Table 2.

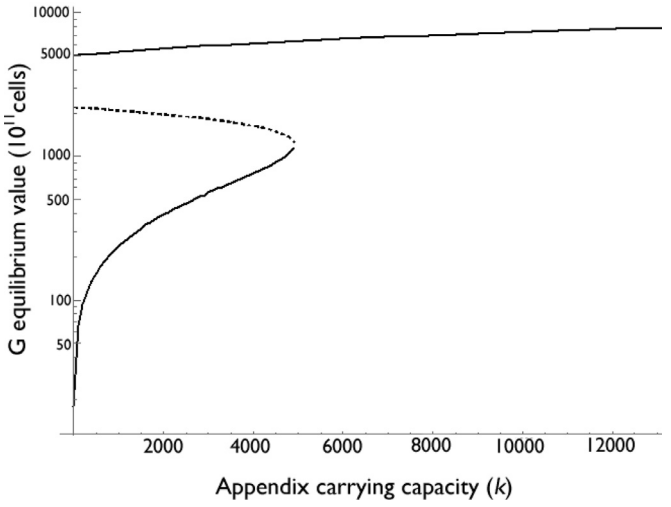

Fig. 7. A bifurcation diagram of the equilibria of G as a function of appendix carrying capacity k. Stable equilibria are denoted with solid lines and the unstable equilibrium with a dashed line. The equilibrium population axis has a logarithmic scale. Parameters used are given in Table 2.

For this parameter set, changing the migration rate of bacteria from the appendix, m, and the boost in antibody production due to the appendix, w, did not change the number of equilibria (Fig. 6). As with the migration-only model, increasing the carrying capacity of the appendix does allow the migration rate to change the number of equilibria present (not pictured for this model; similar to Fig. 3b). For a fixed migration rate, increasing the carrying capacity of the appendix eventually leads to the system moving from bistable to a single healthy steady state (Fig. 7). Again, this only occurs for unrealistically large appendiceal carrying capacities.

3.2. Sensitivity analysis

To explore how this result generalizes in the parameter space, we randomly select 1,000 parameterizations from a uniform distribution within the ranges in Table 2 for all parameters besides m and w. We also evenly divide the ranges for m and w into 10 points each. Then, for each combination of values for m and w, we calculate the number of non-negative equilibria for each parameterization. This resulted in exploring equilibrial dynamics across 100,000 distinct parameter combinations.

Of 1,000 parameter sets for each of the 10 associated values for m and w, varying w and m changed the number of equilibria in only one and thirteen parameterizations respectively. Given the rarity of this behavior, we conclude that the qualitative dynamics of the gut microbiome are generally insensitive to the presence of the appendix (values of m and w). Across the 1,000 parameter sets, both bistability and a single steady state were possible for every value of m and w, further indicating that it is the other parameters and neither the migration rate m nor the antibody production w that shape the qualitative, equilibrium behavior of the model.

To build on these findings, we model the sensitivity of the ultimate outcome—CDI or a healthy host state—to parameter values using regional sensitivity analysis (RSA). RSA (Spear and Hornberger, 1980; Young et al., 1978) partitions input parameter sets into two separate groups, depending on which outcome they lead to. Then, we use the Kolmogorov–Smirnov statistical test, which is the maximum value difference (MVD) between the empirical cumulative distribution functions for each group, as our sensitivity metric (Kottegoda and Rosso, 1997). Parameterizations were chosen using pseudo-random Latin Hypercube sampling to better capture the real variability of the high-dimensional space. The convergence of our sensitivity indices as sample sizes increase provides evidence that the sample size used ($n = 20,000$) is sufficient for stabilization of MVD values (Appendix E). All global sensitivity analyses were conducted using the open-source Sensitivity Analysis For Everybody (SAFE) toolbox (Pianosi et al., 2015).

The main drivers that affect the end state of the system are competition coefficients (f, d), initial conditions for G and C, the relative effect of *C. difficile* bacteria on inflammation (β), the rate that inflammation kills good bacteria (q_G), the *C. difficile* growth rate (z) and the inflammation decay rate (h_I) (Fig. 8). In contrast, the overall outcome is much less dependent on bacterial migration (m) and even less affected by appendiceal antibody production (w).

Finally, we note that we may affect the number of equilibria for the system by changing the inflammation-mediated killing rates (q_C and q_G). Depending on the choice of these values, the migration-inflammation system can either have one healthy steady state or the full bistable equilibrium structure (Fig. 9).

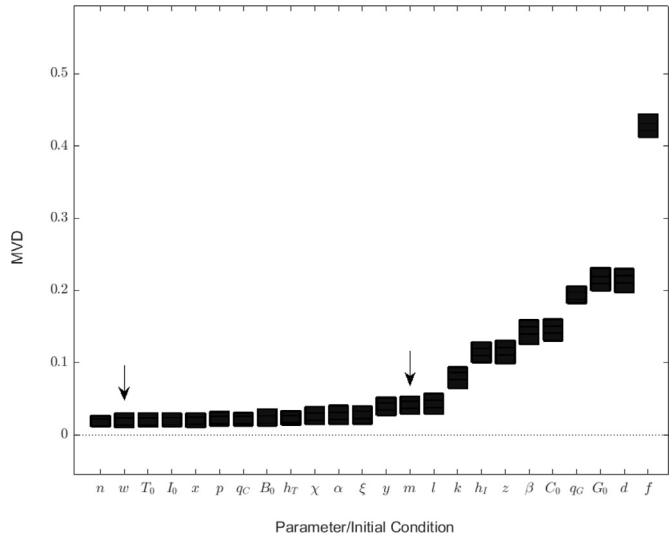

Fig. 8. A plot of the maximum value distance (MVD) between empirical cumulative distribution functions for each parameter and initial condition of the migration-inflammation model, comparing the difference in parameter sets leading to CDI or to a healthy state at 100 days ($n = 20,000$). The MVD is the measure of sensitivity in this regional sensitivity analysis. The box for each parameter is centered around the MVD with the width of the box representing the 95% confidence interval, which is calculated by bootstrapping. Arrows point out the parameters which account for appendix presence.

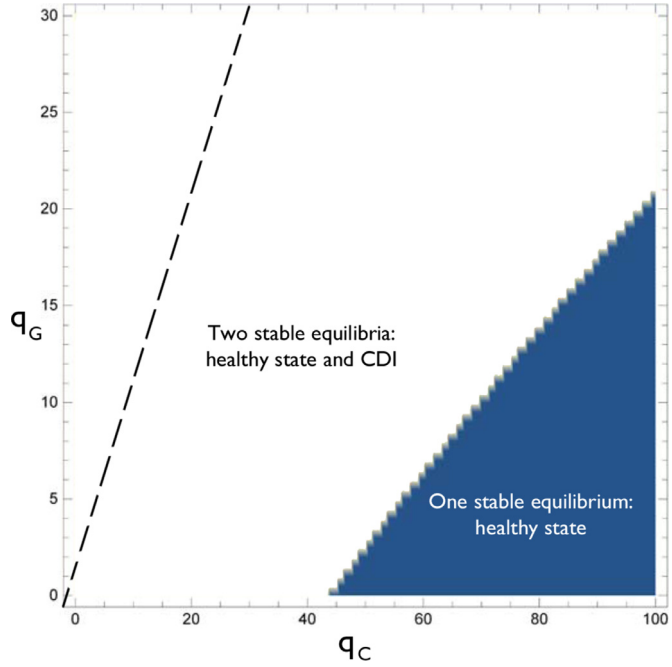

Fig. 9. The number and type of equilibria of system (8)–(12) under the parameter set given in Table 2 for varying inflammation parameters q_G and q_C. The dashed line is a plot of $q_C = q_G$ while the boundary between the two areas demarks the location of the saddle-node bifurcation.

4. Discussion

4.1. Summary

The migration-only model suggests that changes in the appendiceal migration rate do not affect the long-term health of a patient with CDI. We expand upon this result in the migration-inflammation model in which the appendix influences gut bacterial dynamics through the physical migration of cells (m) and the boost to antibody production (w). A regional sensitivity analysis revealed that in the rare situation where appendix presence does have an effect, the change is more likely to occur through antibody production than through the migration of cells (Fig. 8). However, both of these parameters, with biologically realistic values, do not qualitatively affect the stability or number of equilibria for the system in over 99% of examined cases. Thus, we are unable to support the hypothesis that either migration from or the boost in antibody production by the appendix protects against CDI.

Notably, the appendix was simply too small to have a discernible effect on system stability through migration. If the appendix were 1,000 times larger, then changing the migration rate could alter whether the host is susceptible to CDI (Figs. 3 and 7).

Both models exhibit bistability. In general, the goal of treatment is to move from the infected to healthy steady state, as depicted in Fig. 5. If we visualize the system's state on this map for a patient, antimicrobial treatment will kill both *C. difficile* and good bacteria, moving the state down and to the left. Probiotics or fecal transplants will move the state of the system to the right on the figure. Per unit bacteria, killing *C. difficile* bacteria is more effective as a treatment than bolstering the population of good bacteria. Still, this diagram supports a dual treatment for the CDI. This correlates well with our understanding of fecal transplants as an effective mode of treatment for CDI in conjunction with antibiotics (Surawicz et al., 2013).

In addition, we examined the effects of varying the rate of inflammation-mediated killing of cells (Fig. 9). Note from (8), (9) that the effect of multiplying both q_G and q_C by the same factor is the same as multiplying the total inflammation by that factor, so changing the level of inflammation can by visualized as moving parallel to the identity line on this figure. Further, the slope of the identity line is much more steep than that of the bifurcation line. This implies that a decrease in inflammation, such as the result of taking anti-inflammatory medication, could move the system from having both the healthy and ill steady-states to only the healthy steady-state. Thus, the anti-inflammatory drug may protect against CDI.

4.2. Model limitations and extensions

This model is phenomenological—it was designed to roughly evaluate by which possible mechanisms the appendix could exert a realistic effect on CDI. As such, we make several simplifying assumptions, particularly for our treatment of inflammation. Inflammation has a constant decay rate in our model. Also, we ignored any lag time in the production of antibodies after exposure to pathogenic *C. difficile*.

We assume that the rate of *C. difficile* toxin production is simply proportional to the total bacterial population, and does not change when the cell is stressed due to nutrient deprivation (at large population sizes) or due to attack (from inflammation). A few investigations have examined the rate of *C. difficile* bacterial toxin production. In vitro studies have found that toxin expression may be enhanced by stresses such as antibiotics and catabolite repression (Dupuy and Sonenshein, 1998; Onderdonk et al., 1979). Limiting biotin does upregulate toxin production in vitro (Yamakawa et al., 1996). However, limiting amino acids and, thus, growth of *C. difficile* does not enhance toxin production (Yamakawa et al., 1994). Due to these mixed findings, we made the proportionality assumption.

Finally, we conclude that anti-inflammatory drugs may protect against CDI (Fig. 9). However, patients who take the NSAID diclofenac, a highly prescribed anti-inflammatory, have increased risks of CDI (Suissa et al., 2012). Still, no correlation was found between NSAID use and CDI for patients taking other non-steroidal

anti-inflammatory drugs, so this increased risk may be a unique effect of that particular drug (Permpalung et al., 2016).

Extensions to this model may include adding stochastic noise, describing inflammation in more mechanistic terms, and/or altering some parameter values with the state of the system. For example, the diarrhea caused by CDI should increase the flow rate of proteins through the colon and decrease the carrying capacity of the gut (by depleting nutrient sources more rapidly).

4.3. Concluding remarks

This work supports the findings of epidemiologists who have been unable to replicate the deleterious effect of appendectomy on CDI recurrence rates (Khanna et al., 2013). Because appendix size was found to limit its impact, perhaps we should be cautious in evaluating other hypothesized links between the appendix and diseases related to inflammation such as inflammatory bowel disease (Sahami et al., 2015) or cardiovascular disease (Janszky et al., 2011), although our work clearly does not make any direct insights about these diseases.

To further understand and intervene effectively in human-microbe relationships, we must continue to study the microbial community. Perhaps a 21st century goal for medical interventions should be to extend the principle of non-maleficence to include minimizing damage to the homeostasis between humans and their microbiota. Additionally, further progress can be made by framing these systems in an ecological context and viewing the microbiome as an ecological community (Costello et al., 2012). Thus, ecological insights gained from studying species interactions, both theoretical and empirical, may be readily applied to the microbiome, whether or not it is contained within the gut, and help move our understanding forward (Coyte et al., 2015; Stein et al., 2013). Theoretical models borrowed from community ecology, like the ones we used here, will likely prove useful in complementing experimental and applied work to achieve a more complete understanding of the principles that underlie community interactions and host-symbiont interactions that promote human health.

Acknowledgments

This research did not receive any specific grant from funding agencies in the public, commercial, or not-for-profit sectors.

We thank thesis committee members Dr. Wanda Strychalski and Dr. Erkki Somersalo for useful suggestions. Special thanks to Dr. Peter Thomas for valuable insight into the system dynamics. Finally, we thank Dr. Robin Snyder, Dr. Chris Stieha, Dr. Chris Moore, Sam Catella, Katie Dixon, Fang Ji, Brian Lerch, and an anonymous reviewer for thoughtful feedback on the project. BDE would also like to acknowledge Ben Elderd for opening the window into the world of CDI.

Conflicts of interest: none.

Appendix A. Non-dimensionalization

Here, we non-dimensionalize system (6)–(7).

We use the substitutions $G = \hat{G}l$, $C = \hat{C}l$ and $t = \hat{t}y^{-1}$ and also introduce the parameters $s = \frac{z}{y}$ and $r = \frac{m}{ly}\bar{A}$. This produces the equations:

$$\frac{d\hat{G}}{d\hat{t}} = \hat{G} - \hat{G}^2 - d\hat{C}\hat{G} + r$$

$$\frac{d\hat{C}}{d\hat{t}} = s\left(\hat{C} - \hat{C}^2 - f\hat{C}\hat{G}\right)$$

While this system can be written with only four parameters, we will prefer to work with the original dimensional model. The reduced system is less biologically interpretable and non-dimensionalizing the full system (8)–(12) requires different substitutions, impeding our ability to synthesize the two models' results. Moreover, while a sensitivity analysis could be performed on the non-dimensional parameters, such an analysis would not be very useful in understanding the effects of the original parameters on CDI progression.

Appendix B. Well behaved solutions to the migration model

B1. Non-negative

Here, we demonstrate that the migration model is non-negative, given non-negative initial conditions. Consider the system $\boldsymbol{Y}' = (G', C') = (f_1(G, C), f_2(G, C))$ defined by (6) and (7). Now, $\boldsymbol{Y}'$ is composed of polynomial expressions so it is continuously differentiable. Then, by the Picard-Lindelöf Existence-Uniqueness Theorem, $\boldsymbol{Y}$ has a unique local solution for every initial condition.

Next, let $\boldsymbol{Y_1}(t) = (G_1(t), C_1(t))$ be an orbit of the system with $C_1(0) = 0$. Since for $C_1 = 0$ we get $\frac{dC}{dt} = 0$, then a solution is $C_1(t) = C_1(0) = 0$ for all $t \geq 0$. Thus, $C = 0$ is an invariant manifold of the system. Now, assume that there is an orbit of the system such that at some time t_*, $C(t_*) < 0$. By continuity of C, then the orbit with positive initial conditions must cross this manifold which contains a different orbit. However, orbits cannot intersect due to the uniqueness result. Thus, no such trajectory exists and C is always non-negative.

For G, if the appendix is not present, then $m\bar{A} = 0$ and the argument for the non-negativity of G is exactly symmetric to that of C above. Otherwise, we assume that $m\bar{A} > 0$. Then, if there is a time t^* such that $G(t^*) = 0$, we find that $\frac{dG}{dt} = m\bar{A} > 0$ at that time. By the continuity of $\frac{dG}{dt}$, there must exist an $\epsilon > 0$ such that $\frac{dG}{dt} > 0$ for all $t \in [t^* - \epsilon, t^* + \epsilon]$, that is, G must be locally increasing whenever $G(t^*) = 0$. Therefore, an orbit with non-negative initial conditions on G will never become negative.

B2. Bounded

As the previous section demonstrated that there is a lower bound on both G and C, here we show that there are upper bounds as well.

Rewrite (7) as:

$$\frac{dC}{dt} = zC\left(1 - \frac{C}{l}\right) - \frac{z}{l}fCG$$

As C and G are nonnegative, the second term is always nonpositive. If $C > l$, then the first term is negative. Thus, $\frac{dC}{dt} < 0$ whenever $C > l$. Thus, C is bounded above.

Similarly, we assume that $G > \max\{\frac{m\bar{A}}{y}, 2l\}$. As $G > 2l$, $(1 - \frac{G}{l}) < 1 - 2 = -1$.

Then, from (6):

$$\begin{aligned}\frac{dG}{dt} &= yG\left(1 - \frac{G}{l}\right) - \frac{y}{l}dCG + m\bar{A} \\ &\leq yG\left(1 - \frac{G}{l}\right) + m\bar{A} \\ &< -yG + m\bar{A} < 0\end{aligned}$$

where we use our assumption that $G > \frac{m\bar{A}}{y}$ in the final step

B3. Non-oscillatory

This two-dimensional system can be shown to have no limiting periodic solutions. Returning to the notation above, let $(G', C') = (f_1(G, C), f_2(G, C))$ in accordance with (6) and (7). Define the function $\Phi[C, G] = -(CG)^{-1}$. Then, on the quarter plane defined by

$C > 0$ and $G > 0$, we have that

$$\frac{\partial \Phi f_1}{\partial G} + \frac{\partial \Phi f_2}{\partial C} = \frac{m\bar{A}}{CG^2} + \frac{y}{Cl} + \frac{z}{Gl} > 0.$$

Thus by the Bendixson–Dulac theorem, there are no periodic solutions to this system in the region.

Appendix C. Parameter values

In Table 2 we summarize the parameter values used throughout this theoretical study. Some of these values were approximated based on empirical studies. However, there were several parameters for which we could not find any values so we had to provide estimates for them. Note that these estimates were varied in wide ranges in the sensitivity analyses (see Table 2), to assess the impact of using imprecise estimates.

- The turnover rate of colonic epithelial cells is known to be 3–5 days and we assume that the appendiceal bacteria have a similar growth rate range (Park et al., 2016). We also assume that the pathogenic *C. difficile* bacteria can grow from half this rate to triple this rate.
- The per capita migration rate m will range from 0 to the maximal growth rate x of the appendiceal bacteria. The simple presence of a bacterial population in the appendix is evidence that in situ population growth exceeds loss to migration.
- We interpret d as follows: one *C. difficile* bacterium has the same depressive effects on good bacterial growth as d good bacteria. Similarly, for f, one additional commensal bacteria has the same competitive effect as f additional good bacteria. We assume that d and f are no more than 10.
- The human colon has a carrying capacity l on order of 10^{14} bacteria (Tancrede, 1992). A mean maximum diameter for the appendix is 8.19 mm and length is 81.11 mm (Willekens et al., 2014). Approximating this as a cylinder, the surface area is 22 cm^2. A mean diameter for the colon is 50 cm and length is 190 cm (Khashab et al., 2009). The same approximation method gives a volume of $33 \cdot 10^3$ cm^2. If an adult appendix has the same density of bacteria as the colon, then the appendix has on order of 10^{11} bacteria.
- Dinoflaggelates in an in vitro study were found to produce toxins at a rate of 10^{-2} to 10^{-1} fmol per day (Albinsson et al., 2014). Absent data from a closer relative, we assume that *C. difficile* has a similar magnitude rate.
- Different components of the inflammatory response decay at different approximate rates. For example, the decay rate of activated phagocytes is 0.12 per h (Coxon et al., 1999) and for nonspecific IgG and IgA antibodies is 0.002 per h (Reynolds et al., 2006). Therefore, we take the overall decay rate of inflammation h_l as being on the same magnitude scale as its components, so its magnitude is between 10^3 and 10^4 per day.
- The association rate constant for an antibody-antigen interaction was found to be $5.65 \cdot 10^4$ per mole-second (Zhuang et al., 2001). This is $4.88 \cdot 10^{-6}$ per day per fmol.
- Mature plasma B cells can produce 2,000 molecules per second which is 0.287 fmol per day (Alberts et al., 2002). If there are between $10^6 - 10^9$ plasma cells in the colon (estimate), then we expect that χ is between $10^5 - 10^8$ fmol.
- The mean flow of luminal contents in the colon is around 20 μm/s (Cremer et al., 2016). The colon has a median length of roughly 150 cm (Saunders et al., 1996). Therefore, a protein will flow through the colon with a mean time of 0.87 days.

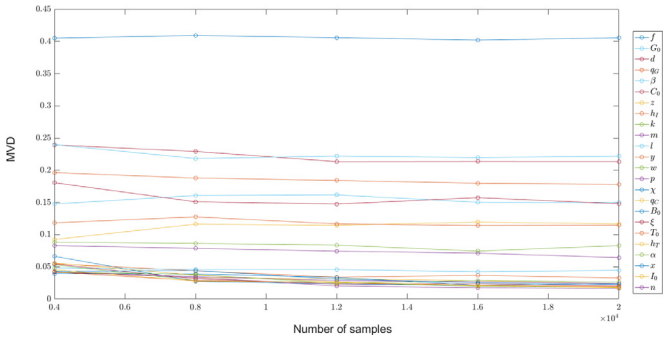

Fig. 10. The maximum value distance (MVD) for each parameter and initial condition of the migration-inflammation model, comparing the difference in parameter sets leading to CDI or to a healthy state at 100 days, as the number of samples increases. The MVD is the measure of sensitivity in this regional sensitivity analysis.

Appendix D. Jacobian matrix for the migration system

The Jacobian matrix for the migration model (6)–(7) is:

$$\begin{bmatrix} y(l - dC - 2\ G) & -dyG \\ -fzC & z(l - 2C - fg) \end{bmatrix}$$

A sufficient condition for the stability of each equilibrium is that the eigenvalues of the Jacobian matrix evaluated at that steady state all have a negative real part.

The eigenvalues corresponding to $e1$ are $\{\sqrt{y}\sqrt{l^2y + 4m\bar{A}}, -\frac{z(-f\sqrt{l^2y+4m\bar{A}}+fl\sqrt{y}-2l\sqrt{y})}{2\sqrt{y}}\}$. Both are real. As the first eigenvalue is always positive, $e1$ is unstable.

The eigenvalues corresponding to $e2$ are $\{-\sqrt{y}\sqrt{l^2y + 4m\bar{A}}, -\frac{z(f\sqrt{l^2y+4m\bar{A}}+fl\sqrt{y}-2l\sqrt{y})}{2\sqrt{y}}\}$. Both are real. The first is negative. The second is negative if and only if either $f \geq 1$ or $f < 1$ and $y < \frac{fm\bar{A}}{(1-f)l^2}$.

For $e3$ and $e4$, the existence and stability conditions of the equilibria are complex expressions of the parameters and we omit them here, although they are present in the supplemental code (Appendix F).

A summary of these results and prior findings about equilibria are presented in Table 1.

Appendix E. Convergence of RSA sensitivity indices

The sensitivity of each parameter and initial condition of the RSA model appears stable in terms of both maximum value distance and relative ranking with a sample size of 20,000 (Fig. 10).

Supplementary material

See supplementary material for Mathematica code giving the non-negativity and stability conditions for equilibria in the migration-only model.

Supplementary material associated with this article can be found, in the online version, at doi:10.1016/j.jtbi.2018.01.013.

References

Alberts, B., Johnson, A., Lewis, J., Raff, M., Roberts, K., Walter, P., 2002. Molecular Biology of the Cell, Fourth Edition. Garland Science.

Albinsson, M.E., Negri, A.P., Blackburn, S.I., Bolch, C.J.S., 2014. Bacterial community affects toxin production by *Gymnodinium catenatum*. PLoS ONE 9 (8), e104623. doi:10.1371/journal.pone.0104623.

Arciero, J.C., Ermentrout, G.B., Upperman, J.S., Vodovotz, Y., Rubin, J.E., 2010. Using a mathematical model to analyze the role of probiotics and inflammation in necrotizing enterocolitis. PLoS One 5 (4), e10066.

Bollinger, R.R., Barbas, A.S., Bush, E.L., Lin, S.S., Parker, W., 2007. Biofilms in the large bowel suggest an apparent function of the human vermiform appendix. J. Theor. Biol. 249 (4), 826–831. doi:10.1016/j.jtbi.2007.08.032.

Bucci, V., Bradde, S., Biroli, G., Xavier, J.B., 2012. Social interaction, noise and antibiotic-mediated switches in the intestinal microbiota. PLoS Comput. Biol. 8 (4), e1002497.

Buffie, C.G., Pamer, E.G., 2013. Microbiota-mediated colonization resistance against intestinal pathogens. Nat. Rev. Immunol. 13 (11), 790–801.

Chieppa, M., Rescigno, M., Huang, A.Y., Germain, R.N., 2006. Dynamic imaging of dendritic cell extension into the small bowel lumen in response to epithelial cell TLR engagement. J. Exp. Med. 203 (13), 2841–2852. doi:10.1084/jem.20061884.

Costello, E.K., Stagaman, K., Dethlefsen, L., Bohannan, B.J., Relman, D.A., 2012. The application of ecological theory toward an understanding of the human microbiome. Science 336 (6086), 1255–1262.

Coxon, A., Tang, T., Mayadas, T.N., 1999. Cytokine-activated endothelial cells delay neutrophil apoptosis in vitro and in vivo. J. Exp. Med. 190 (7), 923–934.

Coyte, K.Z., Schluter, J., Foster, K.R., 2015. The ecology of the microbiome: networks, competition, and stability. Science 350 (6261), 663–666.

Cremer, J., Segota, I., Yang, C., Arnoldini, M., Sauls, J.T., Zhang, Z., Gutierrez, E., Groisman, A., Hwa, T., 2016. Effect of flow and peristaltic mixing on bacterial growth in a gut-like channel. Proc. Natl. Acad. Sci. 113 (41), 11414–11419. doi:10.1073/pnas.1601306113.

DeAngelis, D., Travis, C., Post, W., 1979. Persistence and stability of seed-dispersed species in a patchy environment. Theor. Popul. Biol. 16 (2), 107–125.

Dethlefsen, L., McFall-Ngai, M., Relman, D.A., 2007. An ecological and evolutionary perspective on human–microbe mutualism and disease. Nature 449 (7164), 811–818.

Dupuy, B., Sonenshein, A.L., 1998. Regulated transcription of *Clostridium difficile* toxin genes. Mol. Microbiol. 27 (1), 107–120.

Flint, H.J., 2011. Obesity and the gut microbiota. J. Clin. Gastroenterol. 45, S128–S132.

Im, G.Y., Modayil, R.J., Lin, C.T., Geier, S.J., Katz, D.S., Feuerman, M., Grendell, J.H., 2011. The appendix may protect against *Clostridium difficile* recurrence. Clin. Gastroenter. Hepatology 9 (12), 1072–1077. doi:10.1016/j.cgh.2011.06.006.

Janszky, I., Mukamal, K.J., Dalman, C., Hammar, N., Ahnve, S., 2011. Childhood appendectomy, tonsillectomy, and risk for premature acute myocardial infarction–a nationwide population-based cohort study. Eur. Heart J. 32 (18), 2290–2296. doi:10.1093/eurheartj/ehr137.

Johnson, S., 2009. Recurrent *Clostridium difficile* infection: a review of risk factors, treatments, and outcomes. J. Infect. 58 (6), 403–410. doi:10.1016/j.jinf.2009.03.010.

Johnson, S., Sypura, W.D., Gerding, D.N., Ewing, S.L., Janoff, E.N., 1995. Selective neutralization of a bacterial enterotoxin by serum immunoglobulin A in response to mucosal disease. Infect. Immun. 63 (8), 3166–3173.

Kachrimanidou, M., Malisiovas, N., 2011. *Clostridium difficile* infection: a comprehensive review. Crit. Rev. Microbiol. 37 (3), 178–187. doi:10.3109/1040841x.2011.556598.

Khanna, S., Baddour, L.M., DiBaise, J.K., Pardi, D.S., 2013. Appendectomy is not associated with adverse outcomes in *Clostridium difficile* infection: a population-based study. Am. J. Gastroenterol. 108 (4), 626–627. doi:10.1038/ajg.2012.475.

Khashab, M., Pickhardt, P., Kim, D., Rex, D., 2009. Colorectal anatomy in adults at computed tomography colonography: normal distribution and the effect of age, sex, and body mass index. Endoscopy 41 (08), 674–678.

Kottegoda, N.T., Rosso, R., 1997. Probability, Statistics, and Reliability for Civil and Environmental Engineers. The McGraw-Hill Companies.

Kumar, R., Clermont, G., Vodovotz, Y., Chow, C.C., 2004. The dynamics of acute inflammation. J. Theor. Biol. 230 (2), 145–155.

Larsen, N., Vogensen, F.K., van den Berg, F.W.J., Nielsen, D.S., Andreasen, A.S., Pedersen, B.K., Al-Soud, W.A., Sørensen, S.J., Hansen, L.H., Jakobsen, M., 2010. Gut microbiota in human adults with type 2 diabetes differs from non-diabetic adults. PLoS ONE 5 (2), e9085. doi:10.1371/journal.pone.0009085.

Lessa, F.C., Mu, Y., Bamberg, W.M., Beldavs, Z.G., Dumyati, G.K., Dunn, J.R., Farley, M.M., Holzbauer, S.M., Meek, J.I., Phipps, E.C., et al., 2015. Burden of *Clostridium difficile* infection in the United States. N. Engl. J. Med. 372 (9), 825–834.

McDonald, L.C., Owings, M., Jernigan, D.B., 2006. *Clostridium difficile* infection in patients discharged from US short-stay hospitals, 1996–20031. Emerging Infect. Dis. 12 (3), 409–415. doi:10.3201/eid1205.051064.

Olsen, M.A., Yan, Y., Reske, K.A., Zilberberg, M.D., Dubberke, E.R., 2015. Recurrent *Clostridium difficile* infection is associated with increased mortality. Clin. Microbiol. Infection 21 (2), 164–170.

Onderdonk, A., Lowe, B., Bartlett, J., 1979. Effect of environmental stress on *Clostridium difficile* toxin levels during continuous cultivation. Appl. Environ. Microbiol. 38 (4), 637–641.

Park, J., Kotani, T., Konno, T., Setiawan, J., Kitamura, Y., Imada, S., Usui, Y., Hatano, N., Shinohara, M., Saito, Y., Murata, Y., Matozaki, T., 2016. Promotion of intestinal epithelial cell turnover by commensal bacteria: role of short-chain fatty acids. PLOS ONE 11 (5), e0156334. doi:10.1371/journal.pone.0156334.

Permpalung, N., Upala, S., Sanguankeo, A., Sornprom, S., 2016. Association between NSAIDs and *Clostridium difficile*-associated diarrhea: a systematic review and meta-analysis. Can. J. Gastroenterol. Hepatol. 2016.

Petraitis, P., 2013. Multiple Stable States in Natural Ecosystems. OUP Oxford.

Pianosi, F., Sarrazin, F., Wagener, T., 2015. A matlab toolbox for global sensitivity analysis. Environ. Modell. Software 70, 80–85.

Reynolds, A., Rubin, J., Clermont, G., Day, J., Vodovotz, Y., Ermentrout, G.B., 2006. A reduced mathematical model of the acute inflammatory response: I. Derivation of model and analysis of anti-inflammation. J. Theor. Biol. 242 (1), 220–236. doi:10.1016/j.jtbi.2006.02.016.

Rupnik, M., Wilcox, M.H., Gerding, D.N., 2009. *Clostridium difficile* infection: new developments in epidemiology and pathogenesis. Nat. Rev. Microbiol. 7 (7), 526–536. doi:10.1038/nrmicro2164.

Sahami, S., Kooij, I.A., Meijer, S.L., den Brink, G.R.V., Buskens, C.J., te Velde, A.A., 2015. The link between the appendix and ulcerative colitis: clinical relevance and potential immunological mechanisms. Am. J. Gastroenterol. 111 (2), 163–169. doi:10.1038/ajg.2015.301.

Saunders, B.P., Fukumoto, M., Halligan, S., Jobling, C., Moussa, M.E., Bartram, C.I., Williams, C.B., 1996. Why is colonoscopy more difficult in women? Gastrointest. Endosc. 43 (2), 124–126.

Seretis, C., Seretis, F., Goonetilleke, K., 2014. Appendicectomy and *Clostridium difficile* infection: Is there a link? J. Clin. Med. Res. 6 (4), 239–241. doi:10.14740/jocmr1840w.

Solomon, K., 2013. The host immune response to *Clostridium difficile* infection. Ther. Adv. Infect. Dis. 1 (1), 19–35. doi:10.1177/2049936112472173.

Spear, R., Hornberger, G., 1980. Eutrophication in peel inlet II. Identification of critical uncertainties via generalized sensitivity analysis. Water Res. 14 (1), 43–49.

Spigaglia, P., 2016. Recent advances in the understanding of antibiotic resistance in *Clostridium difficile* infection. Ther. Adv. Infect. Dis. 3 (1), 23–42. doi:10.1177/2049936115622891.

Stein, R.R., Bucci, V., Toussaint, N.C., Buffie, C.G., Rätsch, G., Pamer, E.G., Sander, C., Xavier, J.B., 2013. Ecological modeling from time-series inference: insight into dynamics and stability of intestinal microbiota. PLoS Computat. Biol. 9 (12), e1003388. doi:10.1371/journal.pcbi.1003388.

Suissa, D., Delaney, J.A.C., Dial, S., Brassard, P., 2012. Non-steroidal anti-inflammatory drugs and the risk of *Clostridium difficile*-associated disease. Br. J. Clin. Pharmacol. 74 (2), 370–375. doi:10.1111/j.1365-2125.2012.04191.x.

Surawicz, C.M., Brandt, L.J., Binion, D.G., Ananthakrishnan, A.N., Curry, S.R., Gilligan, P.H., McFarland, L.V., Mellow, M., Zuckerbraun, B.S., 2013. Guidelines for diagnosis, treatment, and prevention of *Clostridium difficile* infections. Am. J. Gastroenterol. 108 (4), 478–498. doi:10.1038/ajg.2013.4.

Tancrede, C., 1992. Role of human microflora in health and disease. Eur. J. Clin. Microbiol. Infect. Dis. 11 (11), 1012–1015.

Willekens, I., Peeters, E., De Maeseneer, M., de Mey, J., 2014. The normal appendix on CT: does size matter? PLoS ONE 9 (5), e96476.

Yamakawa, K., Kamiya, S., Meng, X.Q., Karasawa, T., Nakamura, S., 1994. Toxin production by *Clostridium difficile* in a defined medium with limited amino acids. J. Med. Microbiol. 41 (5), 319–323. doi:10.1099/00222615-41-5-319.

Yamakawa, K., Karasawa, T., Ikoma, S., Nakamura, S., 1996. Enhancement of *Clostridium difficile* toxin production in biotin-limited conditions. J. Med. Microbiol. 44 (2), 111–114. doi:10.1099/00222615-44-2-111.

Young, P., Hornberger, G., Spear, R., 1978. Modeling badly defined systems: some further thoughts. In: Proceedings SIMSIG Conference. Australian National University Canberra, pp. 24–32.

Zhuang, G., Katakura, Y., Omasa, T., Kishimoto, M., Suga, K.-I., 2001. Measurement of association rate constant of antibody-antigen interaction in solution based on enzyme-linked immunosorbent assay. J. Biosci. Bioeng. 92 (4), 330–336.